

Communication

Efficient heteronuclear dipolar decoupling in solid-state nuclear magnetic resonance at rotary resonance conditions

Subhradip Paul^a, Venus Singh Mithu^a, Narayanan D. Kurur^{b,*}, P.K. Madhu^{a,*}^a Department of Chemical Sciences, Tata Institute of Fundamental Research, Homi Bhabha Road, Colaba, Mumbai 400 005, India^b Department of Chemistry, Indian Institute of Technology Delhi, Hauz Khas, New Delhi 110 016, India

ARTICLE INFO

Article history:

Received 9 October 2009

Revised 1 December 2009

Available online 21 December 2009

Keywords:

Solid-state NMR

Heteronuclear dipolar decoupling

Magic-angle spinning

TPPM

SPINAL

PISSARRO

Rotary resonance

ABSTRACT

We introduce here a heteronuclear dipolar decoupling scheme in solid-state nuclear magnetic resonance that performs efficiently at the rotary resonance conditions, where otherwise dipolar couplings are re-introduced. Results are shown proving the efficiency of this scheme at two magnetic fields under magic-angle spinning frequencies of 30 and 20 kHz.

© 2009 Elsevier Inc. All rights reserved.

1. Introduction

Heteronuclear dipolar decoupling schemes are made use of in solid-state nuclear magnetic resonance (NMR) experiments whilst observing rare spins, such as ¹³C and ¹⁵N, that are dipolar coupled to the abundant spin ¹H [1]. Several such schemes are currently available, and some of them are, CW [2], TPPM [3], SPINAL [4], XiX [5,6], SW_F-TPPM [7], and PISSARRO [8]. Extensive investigations [9–11] have shown SW_F-TPPM to be better than most of these schemes either in terms of sensitivity or robustness with respect to experimental parameters or both. This is particularly true in the case of decoupler amplitude regimes of more than 50 kHz and magic-angle spinning (MAS) frequencies of 5–30 kHz.

PISSARRO is a recently introduced decoupling scheme with superior performance when the decoupler RF frequency is an integral multiple of the MAS frequency $\nu_1 = n\nu_r$ ($n = 1, 2, \dots$), the so-called rotary resonance (RR) condition [12]. The other decoupling schemes fail at these conditions owing to the recoupling of heteronuclear dipolar interactions. The superior performance of PISSARRO is attributed to the quenching of the RR effects and it is most suitable at $n = 2$ RR condition [8]. It is noteworthy that the combination of currently achievable MAS frequencies in excess of 70 kHz and the gathering interest in decoupling at lower radio-

frequency amplitudes makes the RR conditions, especially the $n = 1$ and 2 conditions, appear in an increasing number of experimental situations. Further, the RR condition is not narrow banded. RR conditions are also encountered in double-rotation (DOR) [13] experiments where ¹H decoupling has typical values of 15–20 kHz and the MAS frequencies are of the order of 6–9 kHz [14]. Hence, it is very important to understand the reasons behind the efficiency of PISSARRO and at the same time, if possible, try to improve it.

We discovered empirically that simple modifications to the TPPM scheme lead to remarkable decoupling at rotary resonance, which is reported here. Experiments are reported on a sample of uniformly labelled glycine and results compared with PISSARRO at RR conditions. Numerical results are also shown to corroborate the experimental observations.

2. Results and discussions

The scheme that we propose in and around the RR condition is similar to TPPM except that the flip angle of the pulses has a linear dependence on the RF amplitude (compared to $\approx \pi$ in conventional TPPM) and a phase difference of 150° (compared to $\approx 15^\circ$ in conventional TPPM). We refer to this scheme as high-phase TPPM. The pulse duration needs to be optimised between 4 and 6 μ s for all the RF amplitudes at the spinning frequency of 30 kHz. In the experiments reported here, the pulse duration τ_p of PISSARRO in terms of the rotor period τ_r , $\frac{\tau_p}{\tau_r}$ was found to be in the range of 0.2–0.4.

* Corresponding authors. Fax: +91 22 2280 4610 (P.K. Madhu).

E-mail addresses: nkurur@chemistry.iitd.ernet.in (N.D. Kurur), madhu@tifr.res.in (P.K. Madhu).

Fig. 1 shows the comparison between PISSARRO and high-phase TPPM at two MAS frequencies of 30 and 20 kHz and $\nu_1 = \nu_r$ and $\nu_1 = 2\nu_r$ RR conditions. The spectrometer frequency for ^1H was 500 MHz. The CH_2 resonance of uniformly labelled glycine is plotted in the figure. Fig. 2 has the results at a ^1H resonance frequency of 700 MHz. The better efficiency of the high-phase TPPM over PISSARRO is evident from these figures. Fig. 2 further emphasises on the fact that, at high magnetic fields, with the increase of chemical-shift anisotropy value, the performance of the high-phase TPPM is still better than PISSARRO. It is observed that at higher orders of RR conditions ($n > 2$), performance of the high-phase TPPM deteriorates, but remains marginally better than PISSARRO.

Simulations performed with the SPINEVOLUTION programme [15] using the crystallographic coordinates of α -glycine [16] and a ^1H CSA of 2.5 kHz [17,18] confirm our experimental findings. The simulation results in Fig. 3 compare the performance of high-phase TPPM and PISSARRO at two different spinning frequencies, 30 and 20 kHz, and a ^1H Larmor frequency of 500 MHz. From the figure it is clear that the high-phase TPPM delivers a superior performance compared to PISSARRO and the performance of both these sequences worsens with a decrease of spinning frequency.

The simulated intensity variation of the CH_2 peak in the $^{13}\text{CHH}_2$ fragment as a function of pulse duration and $\nu_1 = \nu_r$ with the phase difference in TPPM fixed at 150° is displayed in Fig. 4. The region

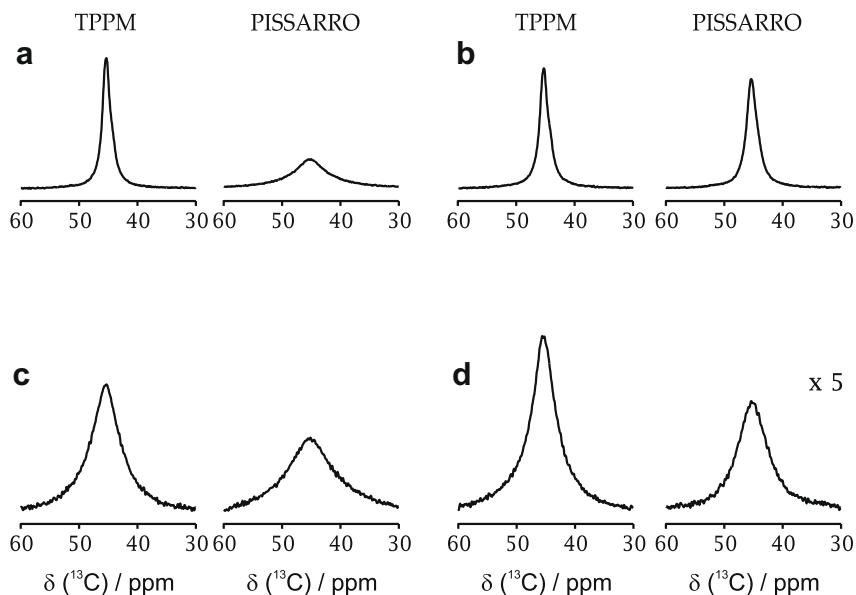


Fig. 1. Spectral comparison of the high-phase TPPM and PISSARRO observing the CH_2 resonance of uniformly labelled glycine for two different MAS frequencies. (a) $\nu_1 = \nu_r = 30$ kHz, (b) $\nu_1 = 2\nu_r = 60$ kHz, (c) $\nu_1 = \nu_r = 20$ kHz, and (d) $\nu_1 = 2\nu_r = 40$ kHz. The RF amplitude levels were calibrated with nutation experiments on a sample of adamantane. The pulse durations in the case of TPPM were (a) 5.4 μs , (b) 4.5 μs , (c) 5.4 μs , and (d) 6 μs . For PISSARRO the optimum pulse durations were (a) $0.4\tau_r$, (b) $0.2\tau_r$, (c) $0.2\tau_r$, and (d) $0.3\tau_r$. The y-axis of the bottom panel is scaled up five times for clarity in intensity comparison. The spectra were obtained on a 500 MHz Bruker AVI NMR spectrometer with a 2.5 mm double resonance probe.

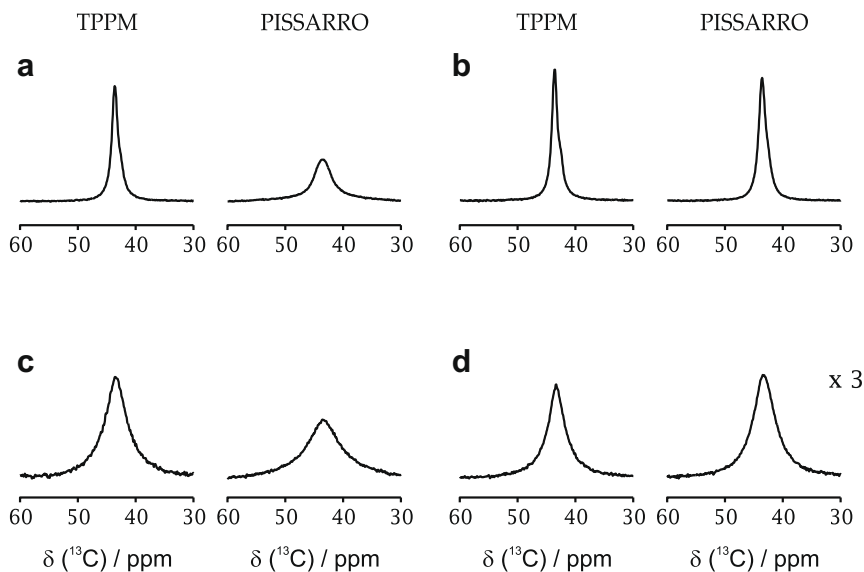


Fig. 2. Same as in Fig. 1 except that the experiments were performed on a 700 MHz Bruker AVIII NMR spectrometer with a 2.5 mm triple resonance probe. The pulse durations in case of high-phase TPPM were (a) 5.2 μs , (b) 5.2 μs , (c) 5.8 μs , and (d) 6 μs . For PISSARRO the optimum pulse durations were (a) $0.2\tau_r$, (b) $0.2\tau_r$, (c) $0.2\tau_r$, and (d) $0.2\tau_r$. The y-axis of the bottom panel is scaled up three times for clarity in intensity comparison.

inside the dotted box is where we have found the best performance for the high-phase TPPM. The efficiency of decoupling improves with higher MAS frequencies. The contour plots clearly demonstrate the superior efficiency of high-phase TPPM over PISSARRO. The contours were simulated with low CSA values so that the powder averaging can be done over a smaller set of Euler angles with

five γ angles. Both experiments and simulations shows that, for a fixed MAS frequency the flip angle for TPPM has a linear dependence with the RF amplitude, approaching 180° at high RF amplitude. These will be presented elsewhere. This observation simplifies the applicability of the sequence as the pulse length has to be optimised for one RF amplitude only.

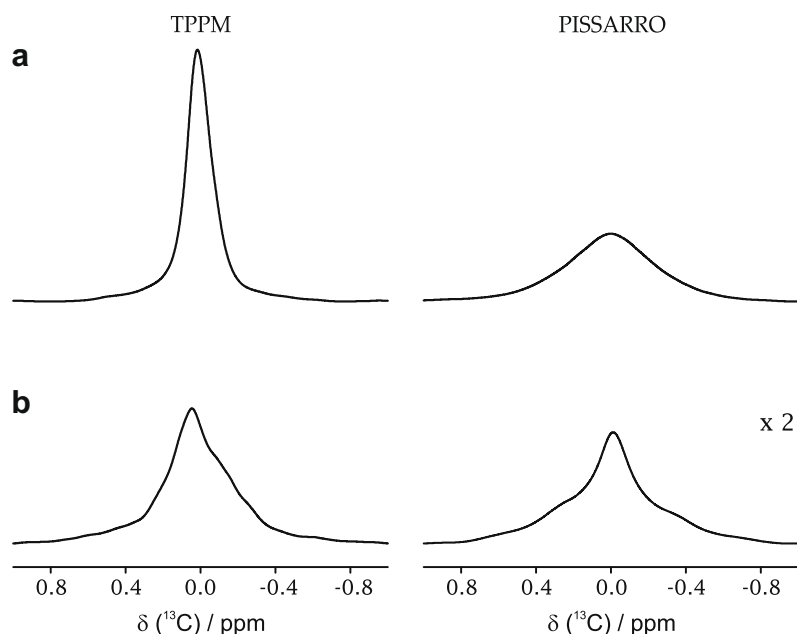


Fig. 3. Simulated spectra of glycine with high-phase TPPM and PISSARRO at spinning frequencies of (a) 30 kHz and (b) 20 kHz with $\nu_1 = \nu_r$. The y-axis of the bottom panel is scaled up two times for clarity in intensity comparison. In the simulations the CH_2 resonance was detected. The simulations were done with 2.5 kHz of CSA on the protons and the ZCW scheme of powder averaging [19–21] with 4181 pair of crystallite orientations. Fifty hertz of line broadening was applied in all the cases in order to emulate relaxation effects.

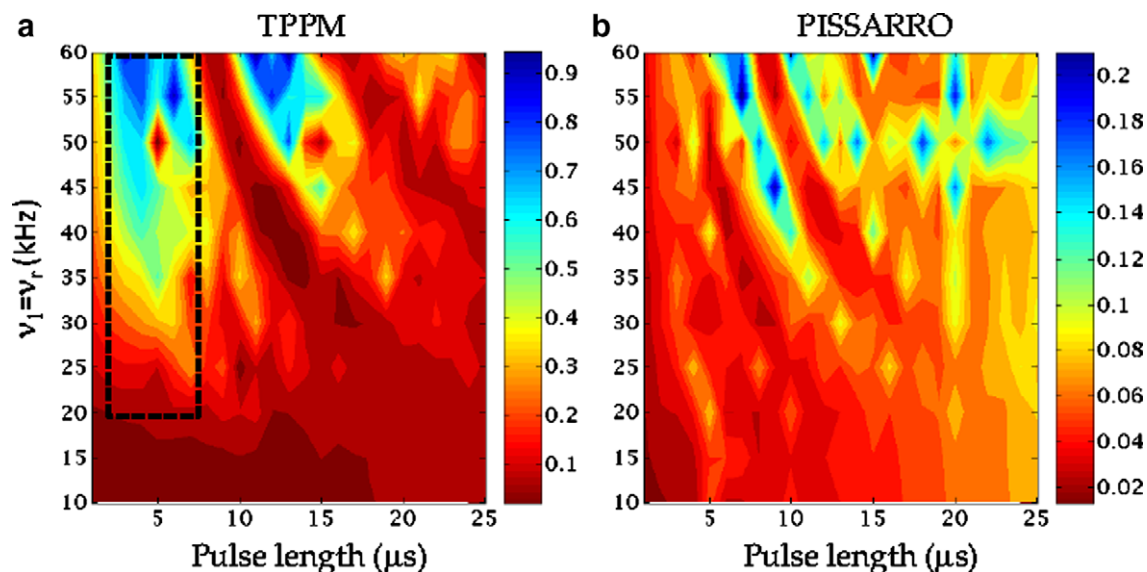


Fig. 4. Contour plots showing the intensity of a $^{13}\text{CH}_2$ system obtained with SPINEVOLUTION programme as a function of the pulse duration and $\nu_1 = \nu_r$ for (a) high-phase TPPM and (b) PISSARRO schemes. The isotropic chemical-shift separation between the H and the H_2 system was 2 ppm and the irradiation frequency on the protons was kept on resonance. The fragment has a dipolar coupling strength of 22 kHz between ^{13}C and two of the protons and 10 kHz with the other proton. The simulations were done with 0.5 kHz CSA on the protons and the ZCW scheme of powder averaging [19–21] with 610 pair of crystallite orientations. The CSA was kept low for the computational constraints of generating the contour plots. The contour levels indicate that the intensity in the case of PISSARRO is only 50% to that of TPPM. The intensities are normalised with respect to the best point obtained with the modified TPPM at $\nu_1 = \nu_r = 60$ kHz. The homonuclear dipolar coupling constant between one of the H in H_2 and H was -23.3 kHz, the second H in H_2 and H was -8.4 kHz, and between the two H in H_2 was -8.6 kHz.

3. Conclusions

We have demonstrated here that two simple modifications of the TPPM scheme result in good decoupling at the investigated RR conditions and outperforms PISSARRO. The high-phase TPPM reported here gives a good performance at the RR conditions of $n = 1$ and 2 whilst PISSARRO gives a good performance at $n = 2$ condition. We are currently investigating the performance of the high-phase TPPM and all other relevant decoupling schemes for a wide range of MAS and decoupler frequency conditions including low decoupler RF amplitude levels.

Acknowledgments

P.K.M. acknowledges assistance from Department of Science and Technology, India, for funding under SERC scheme, SR/S1/PC/27/2009. We acknowledge the National Facility for High Field NMR, TIFR, Mumbai, and technical assistance of M.V. Naik.

References

- [1] M. Mehring, *High Resolution NMR in Solids*, Springer, Berlin, 1976.
- [2] A.L. Bloom, J.N. Shoolery, Effects of perturbing radiofrequency fields on nuclear spin coupling, *Phys. Rev.* 97 (1955) 1261.
- [3] A.E. Bennet, C.M. Rienstra, M. Auger, K.V. Lakshmi, R.G. Griffin, Heteronuclear decoupling in rotating solids, *J. Chem. Phys.* 103 (1995) 6951.
- [4] B.M. Fung, A.K. Khitrin, K. Ermolaev, An improved broadband decoupling sequence for liquid crystals and solids, *J. Magn. Reson.* 142 (2000) 97.
- [5] P. Tekely, P. Palmas, D. Canet, Effect of proton spin exchange on the residual ^{13}C MAS NMR linewidths. Phase-modulated irradiation for efficient heteronuclear decoupling in rapidly rotating solids, *J. Magn. Reson.* A107 (1994) 129.
- [6] A. Detken, E.H. Hardy, M. Ernst, B.H. Meier, Simple and efficient decoupling in magic-angle spinning solid-state NMR: the XiX scheme, *Chem. Phys. Lett.* 356 (2002) 298.
- [7] R.S. Thakur, N.D. Kurur, P.K. Madhu, Swept-frequency two-pulse phase modulation for heteronuclear dipolar decoupling in solid-state NMR, *Chem. Phys. Lett.* 426 (2006) 459.
- [8] M. Weingarth, P. Tekely, G. Bodenhausen, Efficient heteronuclear decoupling by quenching rotary resonance in solid-state NMR, *Chem. Phys. Lett.* 466 (2008) 247.
- [9] M. Leskes, R.S. Thakur, P.K. Madhu, N.D. Kurur, S. Vega, Bimodal Floquet description of heteronuclear dipolar decoupling in solid-state nuclear magnetic resonance, *J. Chem. Phys.* 127 (2007) 024501.
- [10] R.S. Thakur, N.D. Kurur, P.K. Madhu, An analysis of phase-modulated heteronuclear dipolar decoupling sequences in solid-state nuclear magnetic resonance, *J. Magn. Reson.* 193 (2008) 77.
- [11] R.S. Thakur, N.D. Kurur, P.K. Madhu, Pulse duration and phase modulated heteronuclear dipolar decoupling schemes in solid-state NMR, *Proc. Ind. Natl. Sci. Acad.* (2009).
- [12] T.G. Oas, R.G. Griffin, M.H. Levitt, Rotary resonance recoupling of dipolar interactions in solid-state nuclear magnetic resonance spectroscopy, *J. Chem. Phys.* 89 (1988) 692.
- [13] A. Samoson, E. Lippmaa, A. Pines, High resolution solid-state NMR. Averaging of second-order effects by means of a double-rotor, *Mol. Phys.* 65 (1988) 1013.
- [14] R. Dupree, private communication.
- [15] M. Veshtrout, R.G. Griffin, SPINEVOLUTION: a powerful tool for the simulation of solid and liquid state NMR experiments, *J. Magn. Reson.* 178 (2006) 248.
- [16] P. Langan, S.A. Mason, D. Mylesc, B.P. Schoenborn, Structural characterization of crystals of α -glycine during anomalous electrical behaviour, *Acta Crystallogr. B: Struct. Sci.* 58 (2002) 728.
- [17] C. Müller, W. Schajor, H. Zimmerman, U. Haeberlen, Deuteron chemical shift and EFG tensors in α -glycine, *J. Magn. Reson.* 56 (1984) 235.
- [18] D.H. Brouwer, J.A. Ripmeester, Symmetry-based recoupling of proton chemical shift anisotropies in ultrahigh-field solid-state NMR, *J. Magn. Reson.* 185 (2007) 173.
- [19] S.K. Zaremba, Good lattice points, discrepancy, and numerical integration, *Ann. Mater. Pure Appl.* 293 (1966) 4.
- [20] H. Conroy, Molecular Schrödinger equation: VIII. A new method for the evaluation of multidimensional integrals, *J. Chem. Phys.* 47 (1967) 5307.
- [21] V.B. Cheng, H.H. Suzukawa Jr., M. Wolfsberg, Investigations of a nonrandom numerical method for multidimensional integration, *J. Chem. Phys.* 59 (1973) 3992.